Naval Research Laboratory
Stennis Space Center, MS 39529-5004

NRL/MR/7442--98-8084

Validation of the Linear Dispersion Relation Using Field Observations

K. TODD HOLLAND

Mapping, Charting, and Geodesy Branch
Marine Geosciences Division

March 2, 1998

REPORT DOCUMENTATION PAGE

Form Approved
OBM No. 0704-0188

1. AGENCY USE ONLY *(Leave blank)*	2. REPORT DATE	3. REPORT TYPE AND DATES COVERED
	March 2, 1998	Final

4. TITLE AND SUBTITLE

Validation of the Linear Dispersion Relation Using Field Observations

5. FUNDING NUMBERS

Job Order No. 574662008
Program Element No.
Project No. 0603011F
Task No. RDTAF
Accession No.

6. AUTHOR(S)

K. Todd Holland

7. PERFORMING ORGANIZATION NAME(S) AND ADDRESS(ES)

Naval Research Laboratory
Marine Geosciences Division
Stennis Space Center, MS 39529-5004

8. PERFORMING ORGANIZATION REPORT NUMBER

NRL/MR/7442--98-8084

9. SPONSORING/MONITORING AGENCY NAME(S) AND ADDRESS(ES)

Office of Naval Research
800 N. Quincy St.
Arlington, VA 22217-5660

10. SPONSORING/MONITORING AGENCY REPORT NUMBER

11. SUPPLEMENTARY NOTES

12a. DISTRIBUTION/AVAILABILITY STATEMENT

Approved for public release; distribution unlimited

12b. DISTRIBUTION CODE

13. ABSTRACT *(Maximum 200 words)*

The Naval Research Laboratory, working with representatives from the Naval Meteorology and Oceanography Command, the Naval Oceanographic Office, the Office of Naval Research, MEDEA, and MITRE, was tasked to investigate and validate two existing satellite remote sensing methods for determining bathymetry. Both of these methods utilize the linear, finite depth, dispersion equation for surface gravity waves to determine water depth from measurements of wave number magnitude as a function of frequency. Although the main objective of the team's efforts was to quantify the accuracy and efficiency of each method, a secondary task was to identify possible error sources resulting from the use of the dispersion relation under field conditions. This publication describes the results of the dispersion relation validation effort.

Several hundred observations of wave number magnitude for frequencies less than 0.3 Hz were obtained over a wide variety of conditions at the Duck, NC, field site. These data were computed using sophisticated signal processing algorithms that yield precise estimates of wave number that were used to predict water depths assuming the linear dispersion relation. For water depths outside the surf zone region, the results indicate that the linear dispersion relation was highly accurate, with average depth estimation errors on the order of 6% of the observed depth. In shallower regions where wave breaking is evident and nonlinear effects are more pronounced, nominally 4 m and less for Duck, discrepancies between measured and predicted depths of well over 50% were observed. Correlations between the magnitude of the depth error and measured wave amplitudes suggest the importance of wave amplitude in the calculation of shallow-water phase speeds, and correspondingly in the use of the dispersion relation in the surf zone region.

14. SUBJECT TERMS

dispersion relation, wave celerity, cross-spectra, wavenumber

15. NUMBER OF PAGES

25

16. PRICE CODE

17. SECURITY CLASSIFICATION OF REPORT	18. SECURITY CLASSIFICATION OF THIS PAGE	19. SECURITY CLASSIFICATION OF ABSTRACT	20. LIMITATION OF ABSTRACT
Unclassified	Unclassified	Unclassified	SAR

CONTENTS

EXECUTIVE SUMMARY

In 1997, a Bathymetry Integrated Product Team was assembled with representatives from CNMOC, NAVOCEANO, ONR, NRL, MEDEA, and MITRE to investigate and validate two existing satellite remote sensing methods for determining bathymetry. Both of these methods utilize the linear, finite depth, dispersion equation for surface gravity waves to determine water depth from measurements of wavenumber magnitude as a function of frequency. Although the main objective of the team's efforts was to quantify the accuracy and efficiency of each method, a secondary task was to identify possible error sources resulting from the use of the dispersion relation under field conditions. This publication describes the results of the dispersion relation validation effort.

Several hundred observations of wavenumber magnitude for frequencies less than 0.3 Hz were obtained over a wide variety of conditions at the Duck, NC field site. These data were computed using sophisticated signal processing algorithms that yield precise estimates of wavenumber that were used to predict water depths assuming the linear dispersion relation. For water depths outside the surf zone region, the results indicate that the linear dispersion relation was highly accurate, with average depth estimation errors on the order of 6% of the observed depth. In shallower regions where wave breaking is evident and nonlinear effects are more pronounced, nominally 4 m and less for Duck, discrepancies between measured and predicted depths of well over 50% were observed. Correlations between the magnitude of the depth error and measured wave amplitudes suggest the importance of wave amplitude in the calculation of shallow water phase speeds, and correspondingly in the use of the dispersion relation in the surf zone region.

VALIDATION OF THE LINEAR DISPERSION RELATION USING FIELD OBSERVATIONS

1. INTRODUCTION

Determination of water depths stands as an important Naval objective, especially for the success of amphibious and special forces operations near beaches. Since World War II, a variety of remote sensing methods [e.g. *Fuchs*, 1953] have been developed to predict nearshore bathymetric depth contours, most of which rely on a simple, theoretical relation between observable wave characteristics (specifically wavelength and period) and water depth. This relationship is most commonly expressed as the linearized version of the finite depth dispersion equation for surface gravity waves:

$$\sigma = \sqrt{gk \tanh kh} \qquad (1)$$

where the radial frequency, σ, is defined as $2\pi/T$; the magnitude of the wavenumber vector, $k = 2\pi/L$; h is the water depth; T is the wave period; L is the wavelength; and g is the gravitational constant. Note that the solution of (1) for h is direct, given values of σ and k, using the inverse relation

$$h = \frac{\tanh^{-1}\left(\dfrac{\sigma^2}{g\sqrt{k_x^{\,2} + k_y^{\,2}}}\right)}{\sqrt{k_x^{\,2} + k_y^{\,2}}} \qquad (2)$$

with k_x and k_y being the cross-shore and alongshore wavenumber components, respectively.

In 1997, a Bathymetry Integrated Product Team was assembled with representatives from the Naval Meteorology and Oceanography Command, the Naval Oceanographic Office, the Office of Naval Research, the Naval Research Laboratory, MEDEA, and MITRE to investigate and validate two existing satellite remote sensing methods for determining bathymetry. Both of these methods utilize the linear, finite depth, dispersion equation to determine h from measurements of σ and k. Although the main objective of the team's efforts was to quantify the accuracy and efficiency of each method, a secondary task was to identify possible error sources resulting from the use of the dispersion relation under field conditions. A classified document by *Fiedler et. al.*

[1998] presents the main objective findings. This publication describes the results of the dispersion relation validation effort.

1.1. Theory and Assumptions

The partial differential equation governing the irrotational motion of gravity waves at the free surface of an incompressible fluid is known as the Laplace equation. Through the specification of bottom, kinematic free surface, and dynamic free surface boundary conditions, a linear solution is derived for small amplitude waves that are periodic in space and time propagating over a horizontal surface. This solution contains the dispersion relation (1) that identifies the dispersive nature of these type waves, i.e., that longer waves separate from shorter waves in the same wave group by moving faster. It is common to see this relation expressed equivalently in terms of wave celerity or phase speed, c, as

$$c = \frac{\sigma}{k} = \frac{L}{T} = \sqrt{\frac{g}{k}\tanh kh} \qquad (3)$$

In deep water (h is large with respect to L), the equation reduces to $c = {}^{g}\!/_{\sigma}$; and in shallow water, $c^2 = gh$.

In reality, however, the velocity of propagation of nearshore waves is not necessarily independent of wave amplitude. *Stokes* [1847] found a solution for these so-called finite amplitude waves in deep water where the phase speed is governed by k and the wave amplitude, a:

$$c = \sqrt{\frac{g}{k}\left(1 + k^2 a^2\right)} \qquad (4)$$

Stokes's waves are characteristic of many water waves by having a flattened trough and a peaked crest which represents the inherent nonlinear nature of this wave form. Another example of finite amplitude waves, this time in fairly shallow water, is the solitary wave or soliton. This wave, consisting of only a single hump, has a celerity given by

$$c = \sqrt{g(h + a)} \qquad (5)$$

showing that the wave speed increases with the amplitude of the hump [*Stoker*, 1948]. Unfortunately, these nonlinear solutions are of limited use in most bathymetry determination applications because the wave amplitude is a difficult quantity to measure remotely.

In summary, the main assumptions in the linear dispersion relation are that 1) the water depth is constant [i.e. a flat bottom]; 2) the propagating wave train is comprised of uniform, periodic waves; and 3) that the waves are of small amplitude when compared to their wavelength.

Since nearshore bathymetry outside of the breaking region is typically of small slope, the first assumption is somewhat justified. Also, the second assumption that natural wave trains can be approximated by the linear superposition of simple periodic waves has been applied to nearshore hydrodynamics with great success [however, care must be taken in the analysis method to ensure that the individual wave components are accurately quantified]. Finally, using the field observations of this study, the appropriateness of the third assumption will be shown to be somewhat depth dependent.

1.2. Related Research

A number of previous studies have shown the linear dispersion relation remarkably robust in depths typical of nearshore regions and at frequencies typical of incident swell. In moderate depths (8 - 200 m), outside the surf zone region, highly accurate, pressure gauge array measurements have demonstrated deviations of wavenumber observations from predictions using (1) of less than 5% for waves within the frequency range 0.08 - 0.14 Hz [*Herbers and Guza*, 1992; *Herbers and Guza*, 1994; *Herbers et al.*, 1995a; *O'Reilly et al.*, 1996]. Wavenumbers at higher and lower frequencies, showed larger discrepancies which were attributed to either estimator bias or forced-wave contributions to the array cross-spectra. Forced waves, including bounded waves, result from second-order sum or difference interactions of swell and sea; and do not obey a dispersion relationship [for more information see *Okihiro et al.*, 1992; *Herbers and Guza*, 1994; *Herbers et al.*, 1995b].

Using a shore-normal transect of pressure and current sensors, *Thornton and Guza* [1982] computed celerity spectra from pairs of adjacent sensors in depths shoreward of 7-m. Comparison with linear theory showed good agreement to within +20/-10%. These authors also investigated the influence of phase speed advection by mean currents flowing in the onshore-offshore direction. Given the time averaged dominance of offshore flow in many surf zone regions, an increase in the measured celerity compared to that predicted using linear theory would be expected. *Thornton and Guza* [1982] found maximum differences in measured phase speeds that could be attributed to cross-shore flows of 6% and concluded this effect to be insignificant. *Elgar and Guza* [1985], using the same method as *Thornton and Guza* [1982], also found phase speeds slightly greater than linear predictions for observations from Santa Barbara, CA, however, the importance of directional effects including wave reflection on measurements obtained using only shore normal instrumentation was emphasized and cited as a possible cause for the discrepancy. *Elgar and Guza* [1985] state that a 20% increase in wave celerity can result from a reflected component having 10% of the energy of the main wave. For many applications, however, this caution may be unwarranted

as *Elgar et. al.* [1994] showed reflection coefficients are usually below 0.1 for typical incident wave frequencies.

However, finite amplitude effects can not always be excluded in the prediction of wave celerities, especially within the surf zone region. By tracking the displacement of dye by the passage of a single bore, *Inman et. al.* [1971] measured phase speeds bounded by linear and solitary wave theories [Eqns. (3) and (5)] in surf zone water depths of 0.6 to 1.1 m. These authors note that measured values greater than $\sqrt{gh}$ suggest the importance of wave amplitude. *Suhayda and Pettigrew* [1977] showed similar results of phase speed measurements from 10 plunging waves being up to 20% than (5) near the break point and near the shoreline. *Thornton and Guza* [1982] also found apparent finite amplitude effects for waves within the breaking region.

Review of these prior field observations suggests that for waves outside the surf zone at frequencies near the incident spectral peak frequency, the linear predictions given by (2) should be quite accurate. Previous research suggests that inside the surf zone, finite amplitude effects may be important. However, none of these studies has quantified the amount of error introduced by applying the linear dispersion relation over a wide variety of environmental conditions and depths. Given the goal of estimating nearshore bathymetry using remotely sensed dispersion observations, the objective of this report is to accurately define the range of conditions and depths for which the linear approximation is acceptable. In the next section, the field experiments and analysis methods are described. Results are presented in Section 3 and recommendations and conclusions are discussed in the final sections.

2. Field Data and Analysis Methods

2.1. Field Data from the Sampson, Delilah, and Duck94 Experiments

Time series data were collected with bottom-mounted pressure sensor arrays and cross-shore pressure gauge transects at the US Army Corps of Engineers Field Research Facility in Duck, North Carolina [Fig. 1]. The barrier island field site consists of a relatively steep [~1:10] and straight foreshore, one or more longshore sandbars, and an approximately planar offshore region [bottom slope of 1:500] with no nearby headlands or inlets [*Birkemeier et al.*, 1985]. This location is exposed to a range of wave propagation directions and has been categorized as either dissipative or reflective depending on the incident wave conditions [*Holman and Sallenger*, 1985; *Long and Oltman-Shay*, 1991].

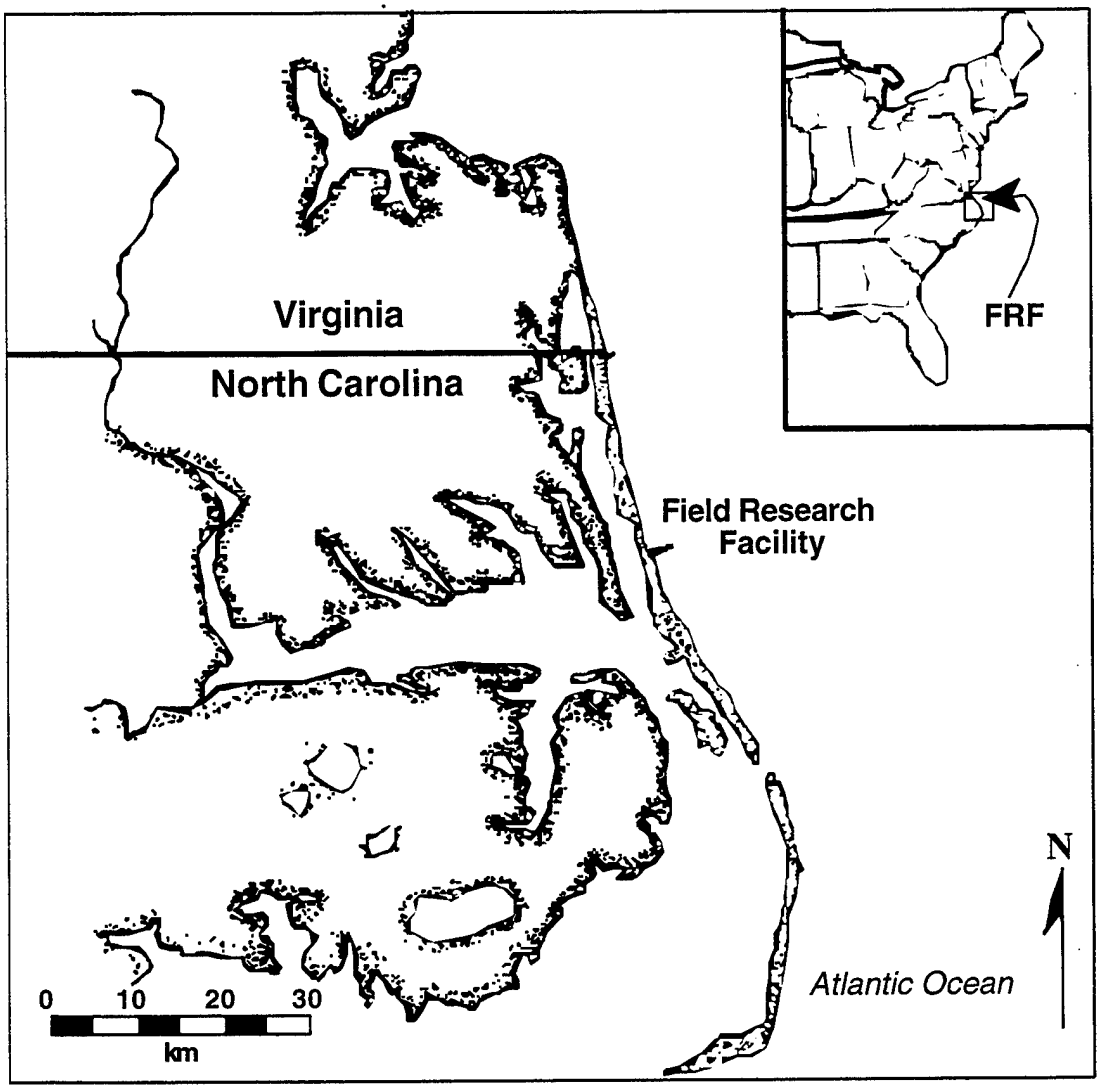

Fig. 1 — Location of field site

The array data were sampled in 8- and 13-m depths [approximately 1 and 2 km from shore, respectively] as part of the Sampson field experiment [data described by *Herbers et al.*, 1994; *Herbers and Guza*, 1994]. The 13-m array consisted of 24 pressure transducers [250 m × 250 m aperture] positioned in a geometric configuration to optimize measurement of theoretically expected wavelengths [Fig. 2]. These data were collected at a 4-Hz sample rate between September 1990 and June 1991 and will be referred to in the following as the Sampson data. Measurements in 8-m depths from a smaller array of 16 sensors [shown in Fig. 3] were made in October, 1990 also at a sample rate of 4 Hz. These data will be referred to as the FRF-8m data. The positioning uncertainties of both arrays were less than 1% of the distance to the array center.

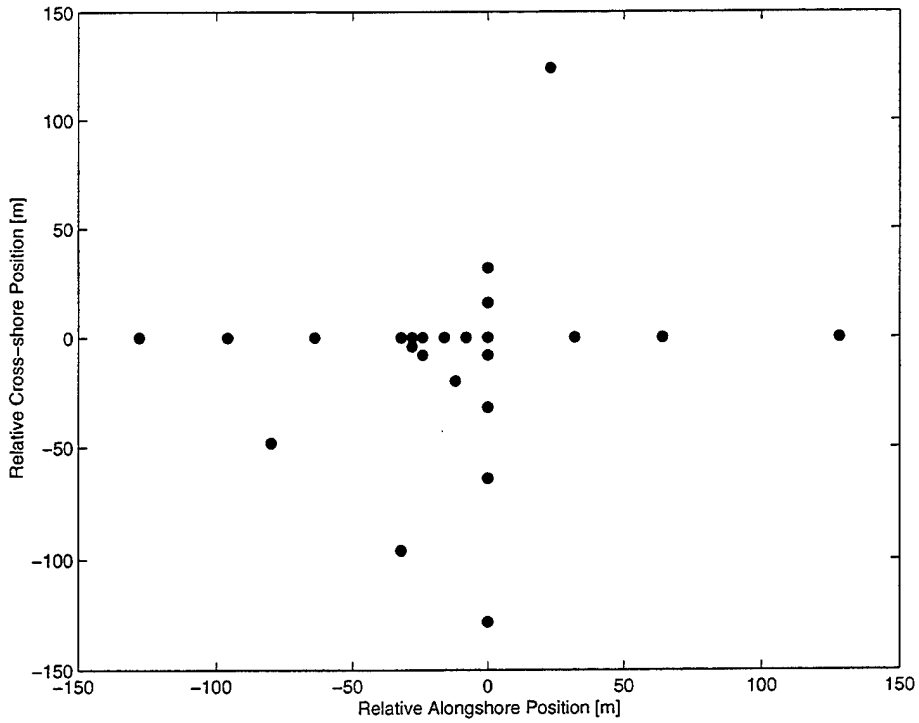

Fig. 2 — Array of pressure sensors (dots) deployed in 13-m depth as part of the Sampson experiment

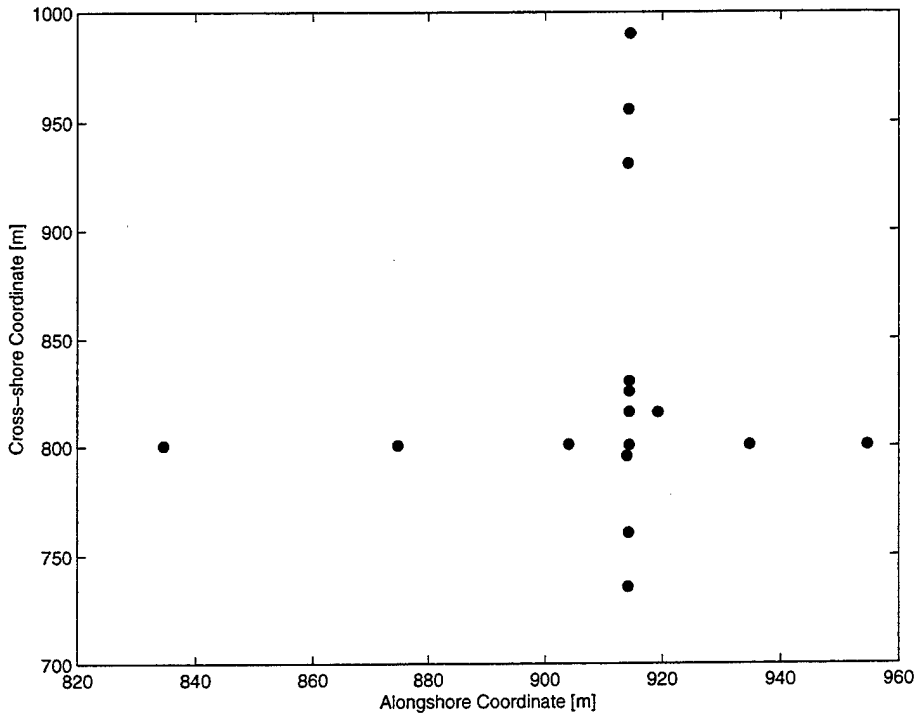

Fig. 3 — FRF sixteen element pressure gage array (dots) deployed in 8-m depth

Additional data were obtained from a linear cross-shore transect of pressure gauges as part of the Delilah and Duck94 experiments [Fig. 4]. The Delilah data were sampled at 8 Hz during the month of October, 1990 and overlap temporally with the FRF-8m data. The Duck94 data were collected at 2 Hz between August and November, 1994. For simplicity, wavenumber estimates were only computed using two pairs of sensors, in depths of 2 and 4 m, respectively. Supplemental measurements, including bottom depth profiles, were derived from the FRF environmental database.

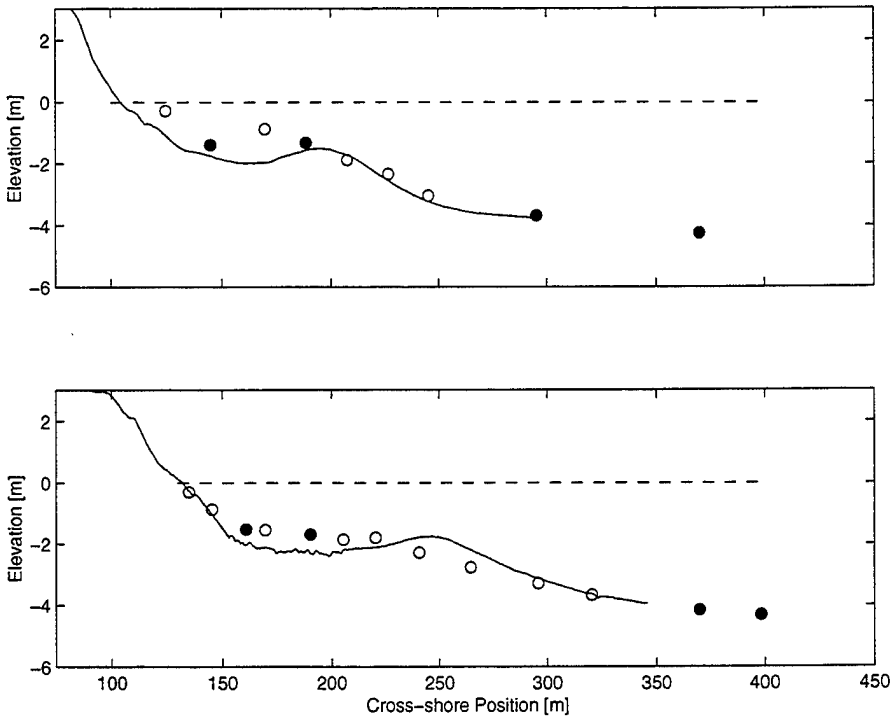

Fig. 4 — Delilah (top) and Duck94 (bottom) cross-shore pressure gage transects: filled circles represent sensors used in this study in approximate depths of 2 and 4 m.

In all, 1,649 data runs were analyzed. The number of runs for the Sampson, FRF-8m, Delilah, and Duck94 data sets were 838, 211, 61, and 539, respectively. The data runs, each 2 hr and 50 min long, consisted of time series measurements from the individual pressure sensors. Estimates of auto-spectra and cross-spectra were obtained from Fourier transforms of the time series, which were detrended [to remove tides], tapered [to minimize leakage], and subdivided into 34 minute ensembles. The final spectral estimates had a frequency resolution of 0.0068 Hz and 140 degrees of freedom. Significant wave heights [defined as 4σ with σ^2 the surface elevation variance in the frequency range 0.06-0.24 Hz] at the 13-m array location ranged between 0.3 and 3.3 m [*Herbers et al.*, 1994].

2.2. *Analysis Methods*

Wavenumber, k, as a function of frequency, f [where $\sigma = 2\pi f$], or equivalently celerity spectra, $c(f)$, is commonly computed using cross spectra between sensor pairs. For the purpose of validation of the linear dispersion relation, the amplitudes of the Fourier components are relatively unimportant compared to the phase information defining the temporal lag of the signal at one gauge relative to the signal at the other. Since this phase difference is essentially a time value, knowing the separation distance between the sensors allows a wave celerity [or equivalent wavenumber for that frequency] to be determined. For the 8-m and 13-m arrays, cross spectra can be computed for all gage pairs assuming the mean depth of all the sensors is approximately equal. Given the large number of independent pairs possible, it is easy to envision that these spatially extensive arrays give a highly accurate estimate of the wavenumber *vector* [both magnitude and direction] as a function of frequency, $\mathbf{k}(f)$. For estimates consisting of measurements from only two sensors, such as with the cross-shore transect instrumentation, only the celerity magnitude in the direction of the array [cross-shore] is derived. Computation of the true celerity requires knowledge of either the alongshore wavenumber, k_y, or incident wave angle at the mean sensor location, θ. Therefore, the analysis of the pressure gauge observations at Duck varies depending on whether the estimates are derived from two closely spaced sensors or from spatially extensive arrays.

2.2.1. Wavenumber estimation using two closely spaced sensors

Squared coherence and celerity spectra were calculated from cross spectra between adjacent pairs of pressure gauges located in a line normal to the beach. Coherence squared, γ^2, and cross-shore celerity, c_x, are defined in (6) and (7) as:

$$\gamma^2(f) = \frac{Co(f)^2 + Qu(f)^2}{C_{11}(f)C_{22}(f)}; \qquad (6)$$

$$c_x(f) = \frac{\sigma \Delta x}{\phi(f)} \qquad \left[\text{Note } k_x = \frac{\phi(f)}{\Delta x}\right] \qquad (7a)$$

where Δx is the distance between sensors, C is the auto-spectrum, Co is the co-spectrum, Qu is the quad-spectrum and ϕ, the phase difference between sensors, is given by

$$\phi(f) = \arctan\left(\frac{Qu(f)}{Co(f)}\right). \qquad (7b)$$

For small angles of wave approach [$\theta < 10°$], $c_x \approx c$ with less than 2% error [*Thornton and Guza*, 1982]. However, when possible, alongshore wavenumber estimates derived from the 8-m array were used to correct for directionality, assuming conservation of k_y. Results were recast in terms of wavenumber estimates for comparison with the offshore array estimates.

An example using this analysis method is shown in Figure 5 for Delilah sensors in approximately 4-m depth on 12 October 1990. The observed energy density spectra for the two sensors used are shown in the upper panel and indicate a frequency of maximum energy of 0.08

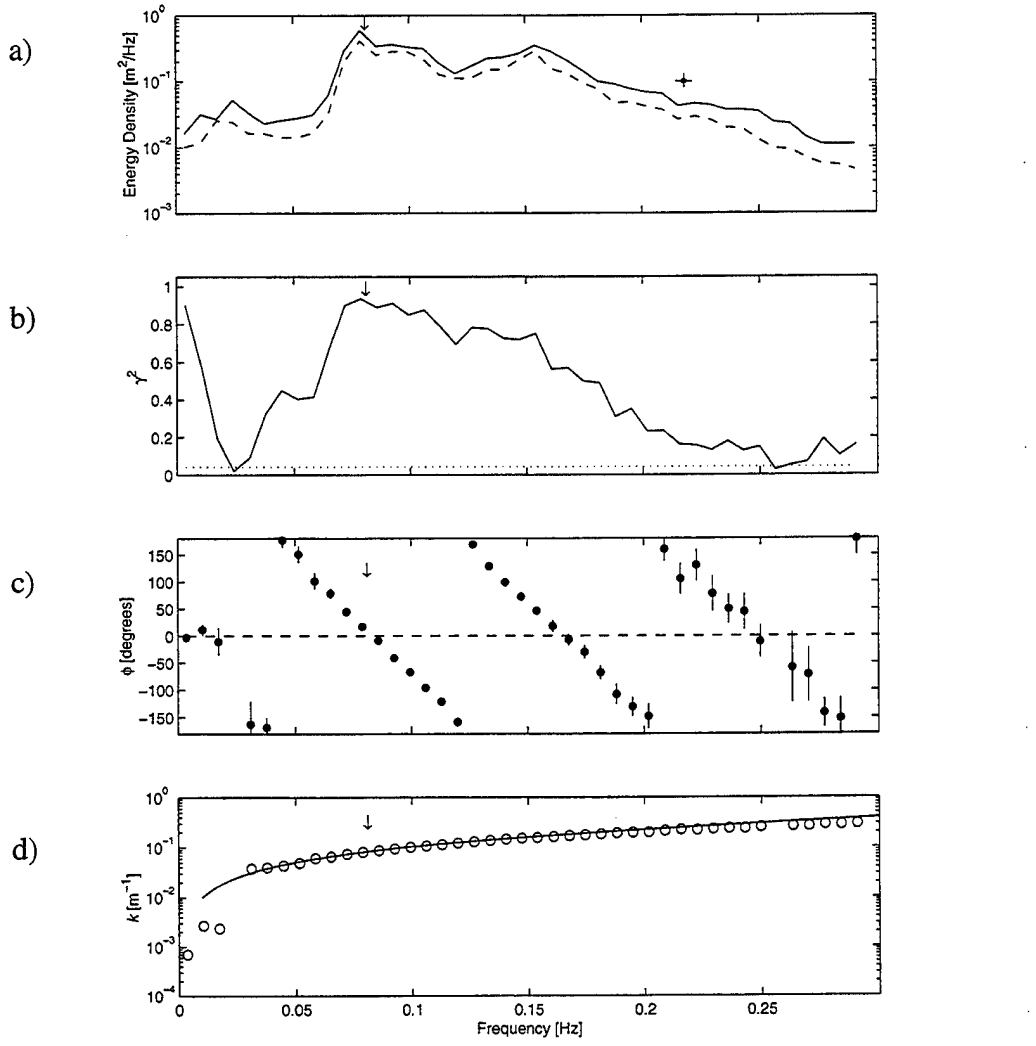

Fig. 5 — Example of a) energy density, b) coherence, c) phase, and d) wavenumber magnitude estimation from measurements in approximately 4m depth on 12 October 1990. The frequency corresponding to the peak in spectral density is indicated by the vertical arrow. The dotted line represents the 95% significance level for coherence. Confidence levels for energy density and phase are also shown.

Hz [denoted by the downward pointing arrow]. A second harmonic is evident at 0.16 Hz. Since the most energetic wave component is also the most likely wave to be apparent in remotely sensed imagery, many of the following results will be referenced in terms of the spectral peak frequency. Coherence at frequencies near the spectral peak [Fig. 5b] was quite high [~0.9] which was typical throughout the experiments of coherence squared estimates in this frequency band. Additionally, the coherence spectrum was used to isolate wavenumber estimates to only significantly coherent signals[*Bendat and Piersol*, 1986]. Phase estimates with error bars are indicated in Figure 5c and show an approximately linear phase ramp suggestive of wave components progressing at a relatively constant phase speed. These phases were used with the sensor separation [75 m in this example] to calculate wavenumber estimates for the observations [Fig. 5d] following (7). Since the confidence intervals [95%] on the phase estimates are quite small, there is minimal error introduced in the cross-shore wavenumber computation due to phase inaccuracy, especially for the frequency band surrounding the spectral peak. The solid line in the lower panel is the wavenumber magnitude predicted using (1) assuming a normally incident wave field and shows good correspondence. Predicted values of wavenumber were determined using the mean depth between sensors including tides. Doppler shifts due to mean cross-shore currents were assumed to be zero.

2.2.2. Estimates using spatially extensive arrays

8- and 13-m results were computed in terms of an estimated root-mean-square average wavenumber, $k_{rms}(f)$ following the estimation technique described by *Herbers et. al.* [1995a]. This method is based on an expansion for small sensor separations relative to the wavelength. The k_{rms} estimate is obtained from a linear combination of normalized cross-spectra

$$k_{rms}^2 = \sum_{p=1}^{N}\sum_{q=1}^{N}\alpha_{pq}\frac{H_{pq}(f)}{\sqrt{H_{pp}(f)H_{qq}(f)}} \tag{8}$$

where $H_{pq}(f)$ is the cross spectrum of a pair of sensors with indices p and q at locations $[x_p, y_p]$ and $[x_q, y_q]$ and N is the number of sensors in the array. Least squares fit solutions for the α_{pq} coefficients were obtained using a singular value decomposition of

$$\begin{aligned}
&\sum_{p=1}^{N}\sum_{q=1}^{N}\alpha_{pq} i^n \frac{(x_p - x_q)^{n-m}(y_p - y_q)^m}{(n-m)!m!} = 1 \\
&\qquad n = 2, m = 0 \;\&\; n = 2, m = 1 \\
&\sum_{p=1}^{N}\sum_{q=1}^{N}\alpha_{pq} i^n \frac{(x_p - x_q)^{n-m}(y_p - y_q)^m}{(n-m)!m!} = 0 \\
&\qquad \text{all other } n, m
\end{aligned} \tag{9}$$

In this analysis the number of terms kept in the expansion was 8 and the truncation value for the smallest eigenvalue [relative to the largest eigenvalue] was 10^{-4} [*Herbers et al.*, 1995a].

3. Results

Figure 6 shows wavenumber estimates and predictions using the above methods for measurements taken on 11 October, 1990 during the Sampson and Delilah experiments. The samples from four depths were temporally coincident and were collected under offshore incident wave conditions of directionally narrow-banded swell with a significant wave height of 1.6 m and a peak period of 9 sec in 8-m depth [Fig. 7]. At the 13-m array, the observations and predictions show excellent agreement for all frequencies less than 0.15 Hz. Estimates in 8-m depths

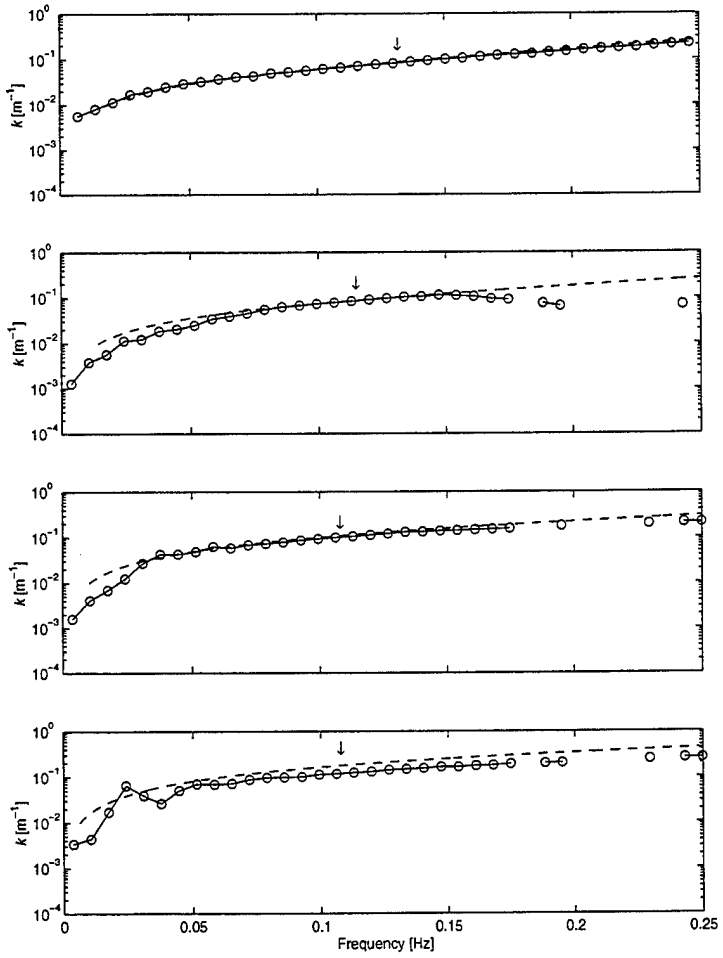

Fig. 6 — Example of wavenumber estimation as a function of frequency at four depths for observations obtained 11 October 1990. Going from top to bottom, the depths corresponding to the four panels are 12.9, 8.1, 4.2 and 1.5 m respectively. Linear theory predictions are indicated by the dashed lines. The downward pointing arrows show a decrease in the spectral peak frequency with decreasing depth.

overlapped closely with predictions over a much smaller frequency range [0.08 - 0.14 Hz] centered about the spectral peak frequency. At 4 and 2 m, the estimated wavenumbers are smaller than predicted for most frequencies and especially at the incident peak. As will be shown next, these results are somewhat typical of the entire set of observations.

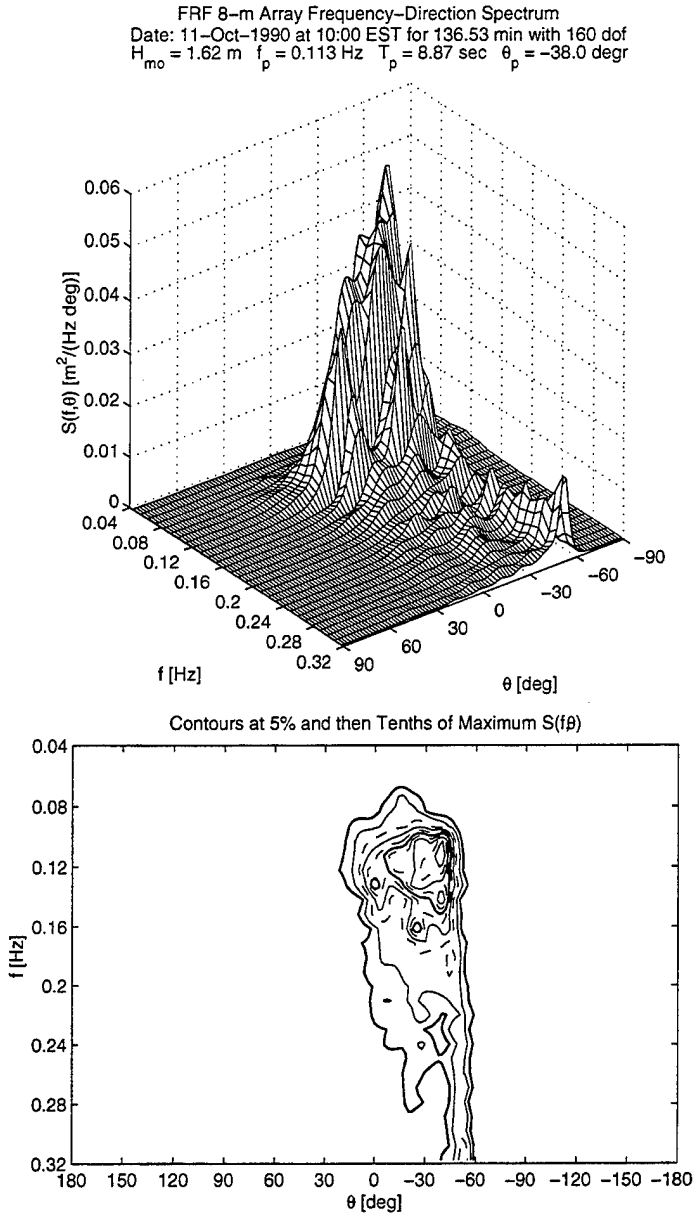

Fig. 7 — Frequency-directional spectrum of wave energy for 11 October 1990

Wavenumber estimates, k_{meas}, at the spectral peak for the entire dataset are presented in Figure 8 relative to theoretical predictions, k_{theory}. Estimates calculated from measurements taken at the 13- and 8-m arrays show excellent correspondence with predictions using the finite depth, linear dispersion equation (1). For these 1049 observations, the average value of the ratio

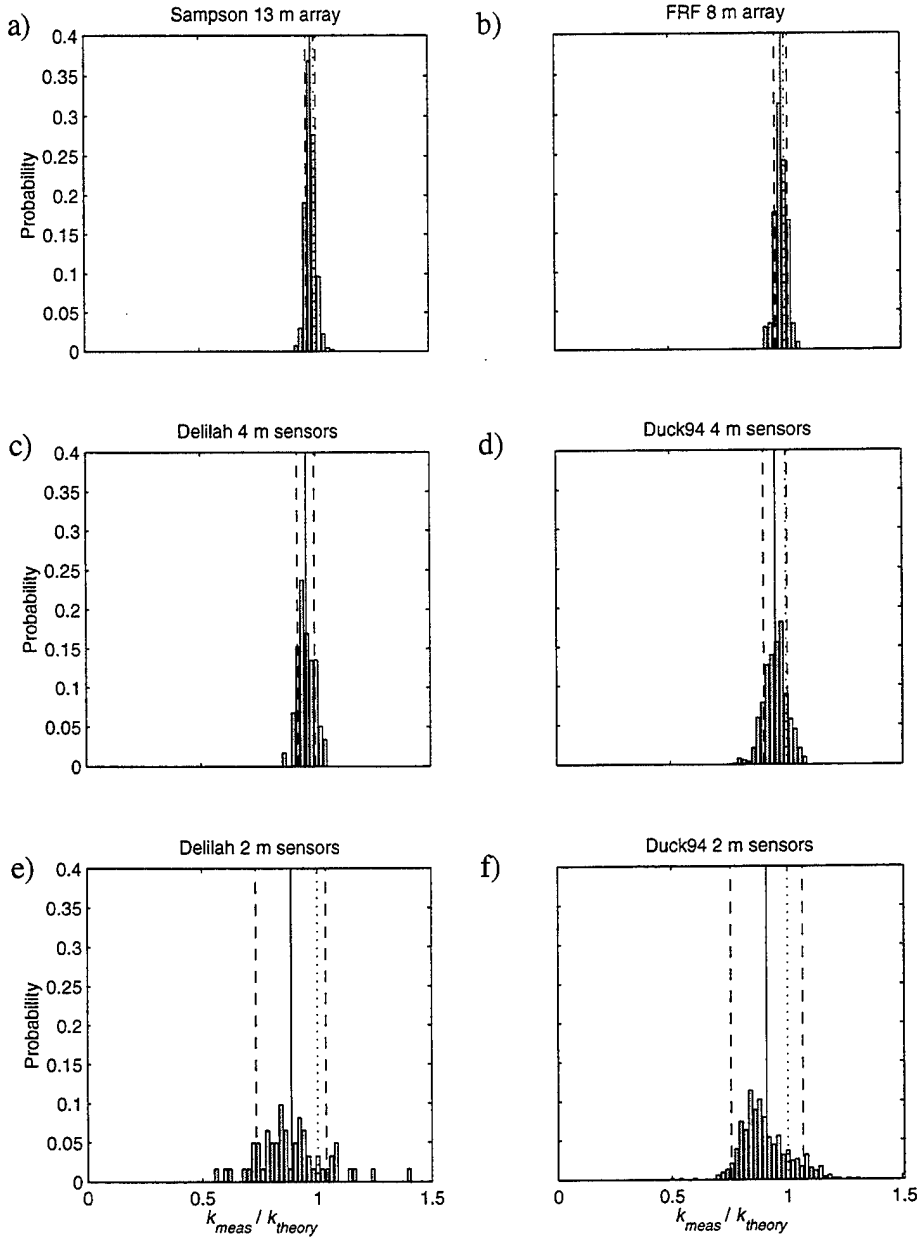

Fig. 8 — Distribution of the ratio of observed to predicted wavenumber magnitudes as a function of depth and experiment. Mean, mean ± one standard deviation, and unity values are represented by the solid, dashed, and dotted lines, respectively.

k_{meas}/k_{theory} was 0.99 indicating a mean deviation of 1%. The standard deviation of the ratio values was 0.02 and the maximum range of deviations was less than ±10%. At 4-m depth [Figs. 8c and 8d], estimates were typically smaller than predictions in that the average value of the above ratio equaled 0.96 for both the Delilah and Duck94 datasets. However, the ranges of this statistic were not dramatically dissimilar to the spread of values for estimates in deeper water [Figs. 8a and 8b]. The standard deviations of the ratio values from the mean ratio value were 0.04 and 0.05 for the Delilah and Duck94 experiment datasets, respectively. The histogram of normalized wavenumber estimates from the most shallow sensors [nominal 2-m depth] was strongly skewed towards small values [Figs 8e and 8f]. The average value of the ratio was 0.88 for the Delilah data and 0.91 for the Duck94 measurements. Standard deviations for both datasets equaled 0.15. Differences between observations and theory at 2 m commonly exceeded 25%. The respective histograms representing Duck94 and Delilah experiment datasets in common depths showed no obvious discrepancies.

The above statistics were recast in terms of absolute depth error, h_{pred} - h_{obs} [Fig. 9], and relative depth error, $\frac{|h_{pred} - h_{obs}|}{h_{obs}}$, where h_{obs} is the observed water depth and h_{pred} is the water depth value predicted using the wavenumber estimates and the inverse dispersion relation (2) [Fig. 10]. The vast majority of the predictions (84%) were found to be greater (deeper) than observed. The mean and modal values of the absolute deviations categorized by approximate depth (13, 8, 4, and 2 m) showed typical bias values on the order of 0.5 m. Average deviations ranged between 0.26 and 0.75 m, with maximum deviations of up to 3 m. The spread of the distributions as approximated by the standard deviation values from the mean was 0.78 at 13 m, 0.52 at 8 m, 0.43

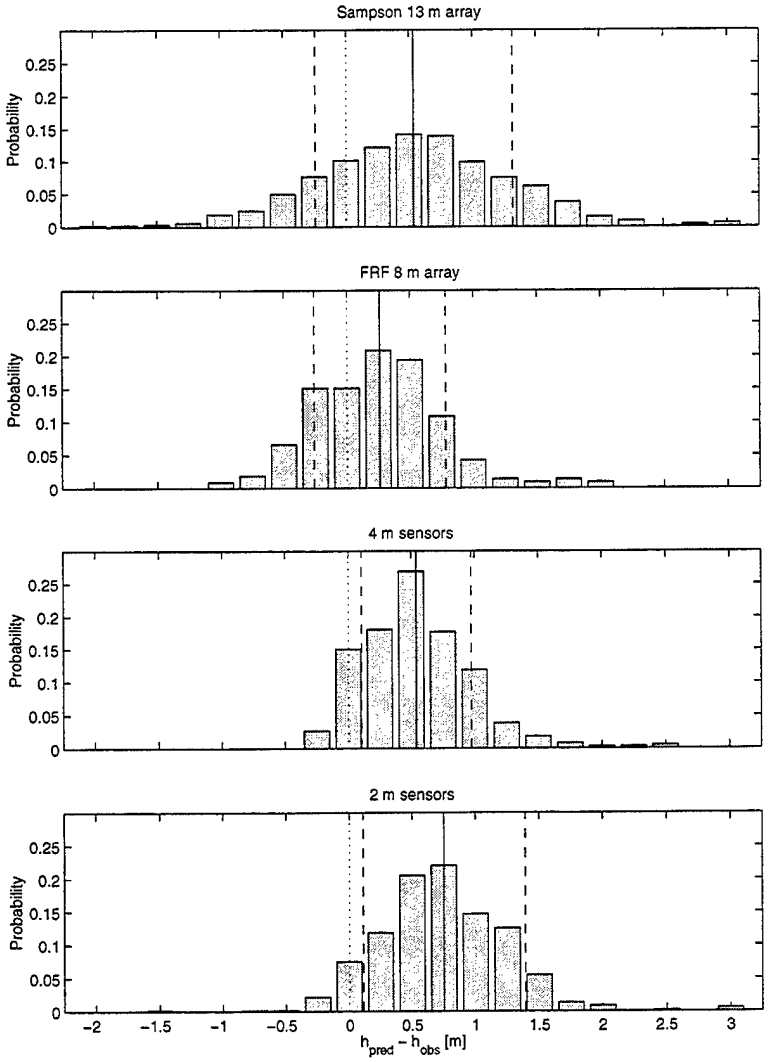

Fig. 9 — Distribution of the absolute depth errors as a function of depth. Mean, mean ± one standard deviation, and zero values are represented by the solid, dashed, and dotted lines, respectively.

at 4 m, and 0.64 at 2 m. Given the more or less constant absolute depth errors [Fig. 10] at the four instrument depths, relative depth errors at the offshore array positions were small compared to errors at shallower depths, with the majority of the observations between 2-8%. Relative errors at the 4- and 2-m sensors, averaged 13% and 41%, respectively.

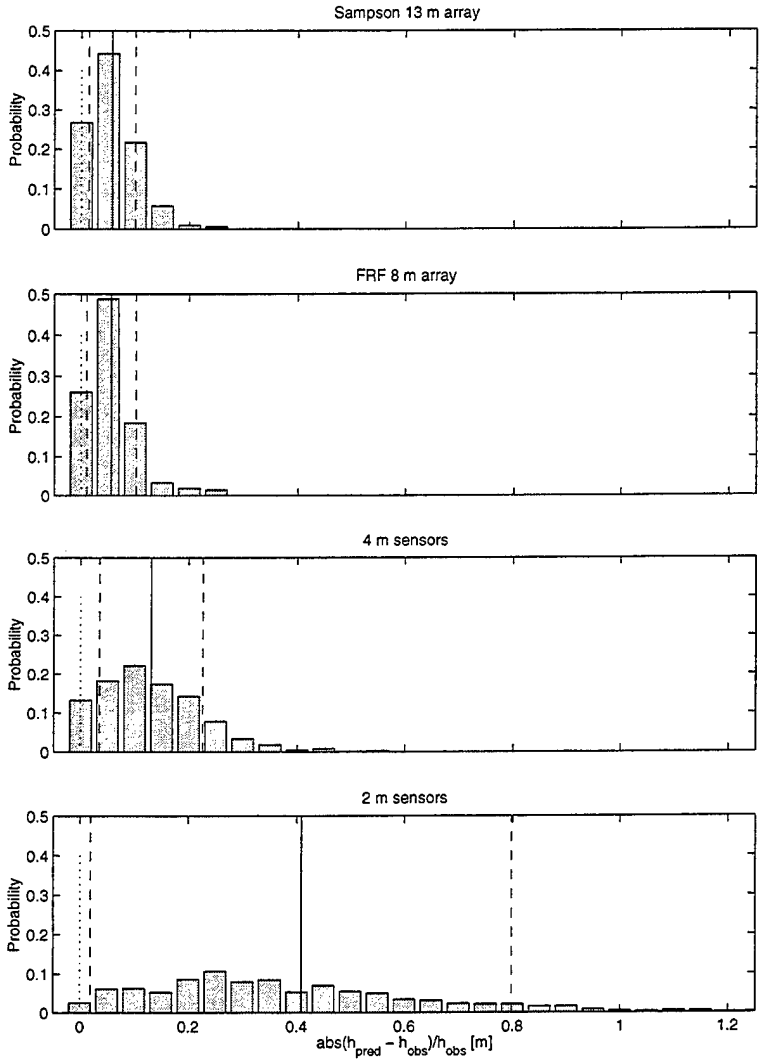

Fig. 10 — Distribution of the relative depth errors as a function of depth. Mean, mean ± one standard deviation, and zero values are represented by the solid, dashed, and dotted lines, respectively.

Figure 11 shows predicted and observed depths using the wavenumber estimates at the spectral peak and (2). The data show good correspondence along a general one-to-one linear trend, however, as indicated previously, the data are markedly offset toward deeper predictions at shallower depths. No systematic differences as a function of analysis method or experiment are apparent.

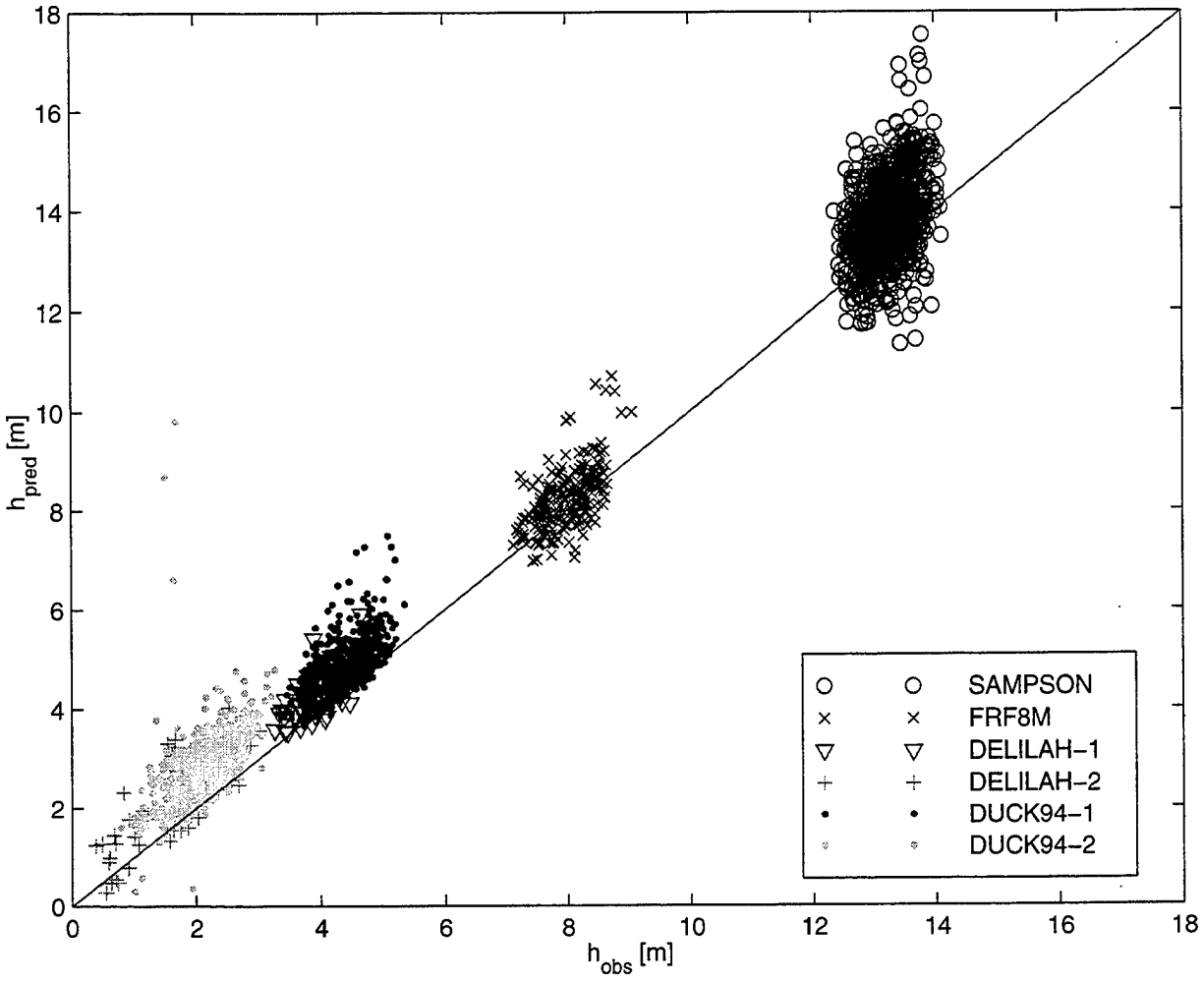

Fig. 11 — Predicted versus observed measurements of depth categorized by experiment. All measurements correspond to values at the spectral peak frequency. A one-to-one line is shown.

4. Discussion

The observations included as part of this report confirm prior findings concerning the appropriateness of using the finite-depth, linear dispersion relation, in nearshore areas including the surf zone. Specifically, for depths outside the breaking region, the approximation was quite good. Average differences between observations and estimates of wavenumber magnitude at the spectral peak frequency were on the order of 1%, with ranges bounding all of the deviations being approximately ±10%. These findings closely mimic the findings of *Herbers and Guza* [1992], *Herbers et. al.* [1994], *Herbers et. al.* [1995a], and *O'Reilly et. al.* [1996]. [Note: *Herbers et. al.* [1994] and *Herbers et. al.* [1995a] used data identical to this study from the Sampson experiment]. Average differences between observations and estimates of water depth were on the order of 6%.

In contrast, for depths near and inside the breaking region (nominally ~ 4 m and less for the Duck site), a strong bias towards overly deep predictions was observed. Depth errors of over 25% for the 4-m measurements and over 50% for the 2-m measurements were common. Overprediction is consistent with several previously suggested possibilities including: directional spreading [*Huang and Tung*, 1977], advection due to cross-shore currents [*Thornton and Guza*, 1982], ignorance of the reflected component in the analysis method [*Elgar and Guza*, 1985], and finite amplitude effects [*Inman et al.*, 1971; *Suhayda and Pettigrew*, 1977; *Thornton and Guza*, 1982].

To investigate the cause of the strong shallow water bias toward deeper predictions, simple correlations between absolute depth error and the following environmental parameters were computed: cross-shore current at the approximate bar crest position, u; significant wave height in 8-m depth, H_{8m}; offshore wave period in 8-m depth, T_{8m}; incidence angle, θ; and a surf-similarity parameter indicative of reflective versus dissipative conditions, ε. No significant linear correlations explaining more than 10% of the observed variance were found for θ, T_{8m}, or ε. This result suggests that any dependence of the errors on processes such as directional spreading or wave

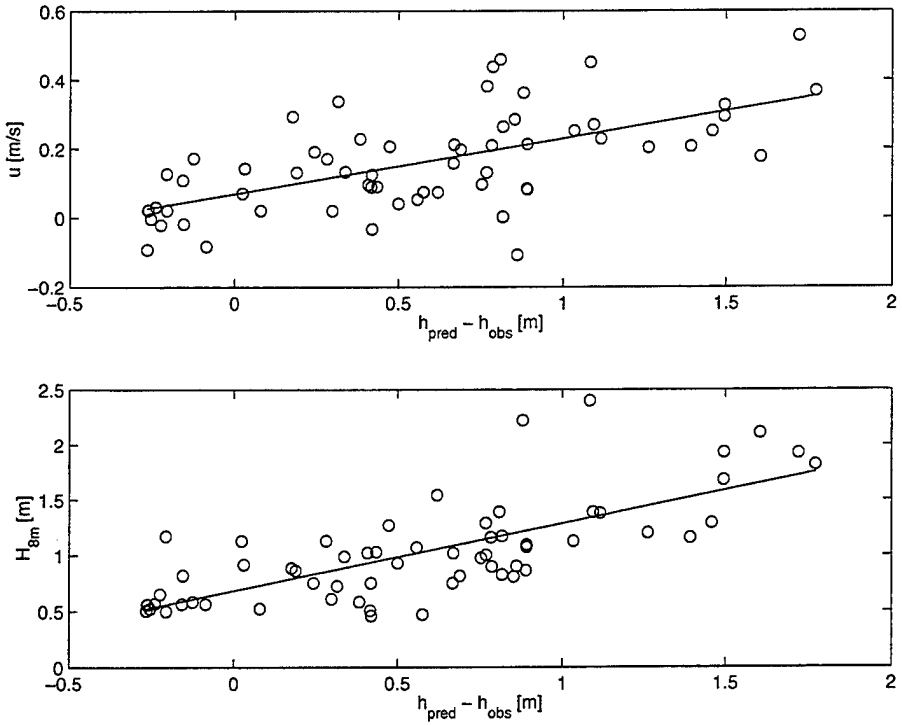

Fig. 12 — Linear correlation between absolute depth error and cross-shore current (top) and significant wave height (bottom). The results are from the Delilah experiment only for measurements in 2-m depth. The correlation coefficients and percentage variance explained for the respective regressions are 0.61, 0.72, 37%, and 52%.

reflection was not resolved through the use of these simplistic parameters. Figure 12a shows significant correlations between cross-shore currents (data obtained only for the Delilah experiment) and absolute errors, especially at the shallowest surf zone depths, however, this correlation could not be uncoupled from an even stronger linear dependence on H_{8m} [Fig. 12b], a likely forcing parameter for cross-shore current behavior. Given that the maximum offshore current value observed [approximately 0.5 m/s] would result in an overprediction of only 20% at these depths, ignorance of Doppler shifts in the measured phase speed could explain only a small portion of the errors [often in excess of 50%].

It is more likely that finite amplitude effects were the primary error source as suggested by the general increase in error with increasing H_{8m}. Comparison of the distribution of depth errors using linear theory [Eqn. (2)] versus solitary wave theory [the depth analog of Eqn. (5)] showed that the overall bias in the predictions can be reduced by more than 0.35 m [42 - 77%] on average by accounting for this type nonlinearity [Figs. 9 and 13]. This finding supports theorized reductions in errors of up to 42%, proposed by *Thornton and Guza* [1982], through the use of solitary wave theory. However the spread of the distributions for the data in this study is largely unchanged suggesting that other presently unexplained factors are important. It is also unclear what size bottom perturbations can be detected using these methods. Both of these questions will be addressed in future work.

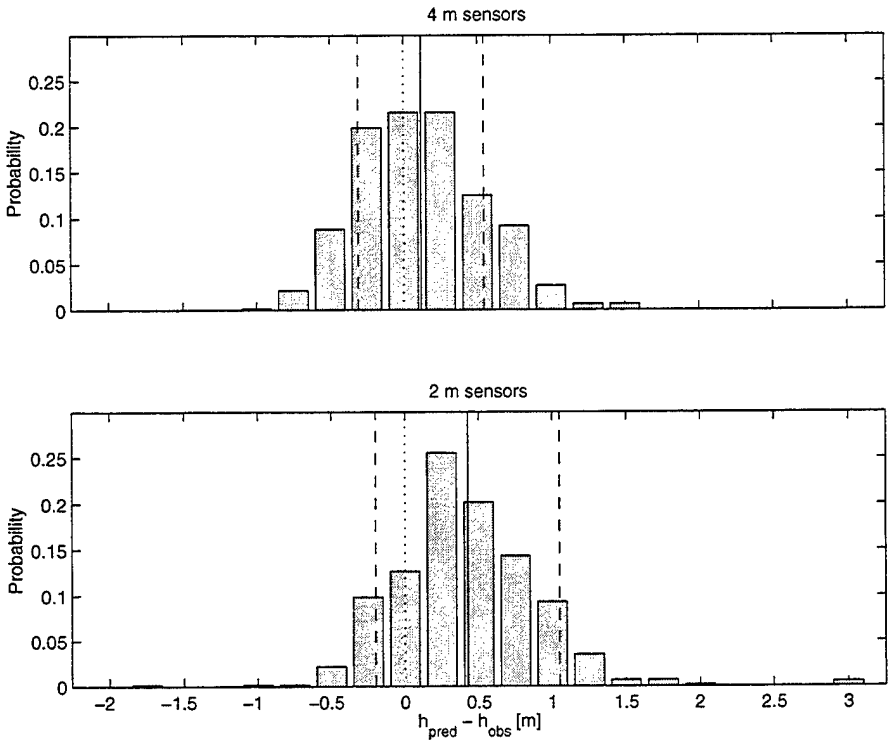

Fig. 13 — Distribution of absolute depth errors computed using solitary wave theory.

5. Summary and Conclusions

Field observations of wavenumber magnitude for frequencies less than 0.3 Hz were obtained to validate the linear version of the finite depth dispersion equation for surface gravity waves. This relation is useful in the estimation of bottom depths using remotely sensed measurements of phase speed or wavenumber magnitude. For water depths outside the surf zone region, the linear dispersion relation was highly accurate, with average depth estimation errors on the order of 6% of the observed depth. In shallower regions [nominally 4 m and less for the Duck site], where wave breaking was evident and nonlinear effects were more pronounced, discrepancies between measured and predicted depths of well over 50% were observed. The results showed overpredictions for the majority of the observations. Correlations between the magnitude of the depth error and measured wave amplitudes suggest the importance of wave amplitude in the calculation of shallow water phase speeds, and correspondingly in the use of the dispersion relation in the surf zone region.

6. Acknowledgments

The author thanks Dr. Tom Herbers of the Naval Postgraduate School for supplying the Sampson 13-m array data; and Dr. Bob Guza of Scripps Institution of Oceanography and Dr. Steve Elgar of Washington State University for providing the Duck94 surf zone sensor time series. The 8-m array and Delilah surf zone array data were provided by the US Army Corps of Engineers' Field Research Facility, specifically through the efforts of Kent Hathaway, Chuck Long, and Cliff Baron. Each of the above also contributed helpful insight on the wavenumber validation study, in general, which was greatly appreciated, as were the comments of Dr. Rob Holman of Oregon State University. This work was funded as part of the National Ocean Partnership Program.

7. References

Bendat, J.S., and A.G. Piersol, *Random Data: Analysis and Measurement Techniques*, 566 pp., Wiley-Interscience, New York, 1986.

Birkemeier, W.A., H.C. Miller, S.D. Wilhelm, A.E. DeWall, and C.S. Gorbics, *A user's guide to the Coastal Engineering Research Center's (CERC's) Field Research Facility*, Instruction Report 85-1, Coastal Engineering Research Center, U.S. Army Corps of Engineers Waterways Experiment Station, pp. 136, 1985.

Elgar, S., and R.T. Guza, Shoaling gravity waves: Comparisons between field observations, linear theory, and a nonlinear model, *J. Fluid Mech.*, *158*, 47-70, 1985.

Elgar, S., T.H.C. Herbers, and R.T. Guza, Reflection of ocean surface gravity waves from a natural beach, *J. Phys. Oceanogr.*, *24* (7), 1503-1511, 1994.

Fuchs, R.A., *Depth estimation on beaches by wave velocity methods*, Series 74 Issue 7, Institute of Engineering Research Wave Research Laboratory, pp. 23, 1953.

Herbers, T.H.C., S. Elgar, and R.T. Guza, Infragravity-frequency (0.005-0.05 Hz) motions on the shelf. Part I: Forced waves, *J. Phys. Oceanogr.*, *24* (5), 917-927, 1994.

Herbers, T.H.C., S. Elgar, and R.T. Guza, Generation and propagation of infragravity waves, *J. Geophys. Res.*, *100* (C12), 24863-24872, 1995a.

Herbers, T.H.C., S. Elgar, R.T. Guza, and W.C. O'Reilly, Infragravity-frequency (0.005-0.05 Hz) motions on the shelf, Part II: Free waves, *J. Phys. Oceanogr.*, *25* (6), 1063-1079, 1995b.

Herbers, T.H.C., and R.T. Guza, Wind-wave nonlinearity observed at the sea floor. Part 2: Wavenumbers and third-order statistics, *J. Phys. Oceanogr.*, *22* (5), 489-504, 1992.

Herbers, T.H.C., and R.T. Guza, Nonlinear wave interactions and high-frequency seafloor pressure, *J. Geophys. Res.*, *99* (C5), 10,035-10,048, 1994.

Holman, R.A., and A.H. Sallenger, Jr., Setup and swash on a natural beach, *J. Geophys. Res.*, *90* (C1), 945-953, 1985.

Huang, N.E., and C.C. Tung, The influence of the directional energy distribution on the nonlinear dispersion relation in a random gravity wave field, *J. Phys. Oceanogr.*, *7*, 403-414, 1977.

Inman, D.L., R.J. Tait, and C.E. Nordstrom, Mixing in the surf zone, *J. Geophys. Res.*, *76* (15), 3493-3514, 1971.

Long, C.E., and J.M. Oltman-Shay, *Directional characteristics of waves in shallow water*, Technical Report CERC-91-1, Coastal Eng. Res. Cent., Field Res. Facil., U. S. Army Eng. Waterw. Exp. Sta., Vicksburg, Miss., pp. 154, 1991.

O'Reilly, W.C., T.H.C. Herbers, R.J. Seymour, and R.T. Guza, A comparison of directional buoy and fixed platform measurements of Pacific swell, *J. Atm. Ocean. Tech.*, *13* (1), 231-238, 1996.

Okihiro, M., R.T. Guza, and R.J. Seymour, Bound infragravity waves, *J. Geophys. Res.*, *97* (C7), 11,453-11,469, 1992.

Stoker, J.J., The formation of breakers and bores, *Communications on Applied Mathematics*, *1* (1), 1-87, 1948.

Stokes, G.G., On the theory of oscillatory waves, *Trans. Camb. Phil. Soc.*, *8*, 441-455, 1847.

Suhayda, I.N., and N.R. Pettigrew, Observations of wave height and wave celerity in the surf zone, *J. Geophys. Res.*, *82* (9), 1419-1424, 1977.

Thornton, E.B., and R.T. Guza, Energy saturation and phase speeds measured on a natural beach, *J. Geophys. Res.*, *87* (C12), 9499-9508, 1982.